Lattice QCD at Imaginary Chemical Potential in the Chiral Limit

D. A. Clarke,[a] **Jishnu Goswami,**[a,*] **F. Karsch,**[a] **Anirban Lahiri,**[a] **M. Neumann**[a] **and C. Schmidt**[a]

[a]*Fakultät für Physik, Universität Bielefeld,*
Bielefeld, Germany
E-mail: dclarke@physik.uni-bielefeld.de, jishnu@physik.uni-bielefeld.de,
karsch@physik.uni-bielefeld.de, alahiri@physik.uni-bielefeld.de,
neumann@physik.uni-bielefeld.de, schmidt@physik.uni-bielefeld.de

We report on an ongoing study on the interplay between Roberge-Weiss (RW) and chiral transitions in simulations of (2+1)-flavor QCD with an imaginary chemical potential. We established that the RW endpoint belongs to the 3-d, $\mathbb{Z}_2$ universality class when calculations are done with the Highly Improved Staggered Quark (HISQ) action in the RW plane with physical quark masses. We also have explored a range of quark masses corresponding to pion mass values, $m_\pi \geq 40$ MeV and found that the transition is consistent with $\mathbb{Z}_2$ universality class. We argue that observables that were usually used to determine the chiral phase transition temperature, e.g. the chiral condensate and chiral susceptibility, are sensitive to the RW transition and are energy-like observables for the $\mathbb{Z}_2$ transition, contrary to the magnetic-like (order parameter) behavior at vanishing chemical potential. Moreover the calculations performed at $m_\pi \sim 40$ MeV also put a stringent constraint for a critical pion mass at zero chemical potential for a possible first-order chiral phase transition.

---

*Speaker

1. Introduction

We are exploring the phase diagram of QCD with two light, degenerate flavors $l \equiv u = d$ and one heavier flavor s, *i.e.* $(2 + 1)$-flavor QCD. This phase diagram depends on the temperature T, chemical potentials μ_f of the various quark flavors f, and their masses m_f. At $m_l = 0$ there is a chiral phase transition, and while it was originally argued to be second-order belonging to the 3-d, O(4) universality class [1], which is supported by recent lattice calculations [2–4], it is also possible that this transition is first-order; indeed finally settling the nature of the chiral transition is still an open issue.

At $\mu_f = 0$ and physical strange quark mass m_s, in the second-order scenario, the transition is O(4) only at $m_l = 0$ and crossover elsewhere. By contrast in the first-order scenario, an m_{crit} exists such that at $m_l = m_{\mathrm{crit}}$ the transition is $\mathbb{Z}_2$, with a first-order region for $m_l < m_{\mathrm{crit}}$. In the case of three degenerate light quark flavors some evidence of this first-order region was found from coarse lattices using an unimproved staggered discretization scheme [5]; however this finding depends strongly on the cutoff [6] and seems to disappear under more highly improved discretizations [7]. This also strongly suggests that the chiral phase transition in $(2 + 1)$-flavor QCD is second order.

The QCD partition function with a purely imaginary chemical potential $\mu = i\mu_I$ is known to exhibit a $\mathbb{Z}_3$ periodicity [8]

$$\mu_I/T \rightarrow \mu_I/T + 2\pi n/3, \tag{1}$$

where $n \in \mathbb{Z}$. Choosing μ_I at the center of this sector, i.e. at $\mu_I/T = (2n + 1)\pi/3$, is the Roberge-Weiss (RW) plane, and we denote the corresponding chemical potential μ_{RW}. In studies where one finds a first-order region, it is also found that $m_{\mathrm{crit}} = m_{\mathrm{crit}}(\mu_I)$ increases with increasing, purely imaginary chemical potential [9]. This m_{crit} is largest at $m_{\mathrm{crit}}(\mu_{\mathrm{RW}})$; therefore in the context of looking out for the previously mentioned first-order region, it is useful to look out for this m_{crit} in the RW plane, which can then be used to place an upper bound on $m_{\mathrm{crit}}(0)$.

Two possible phase diagrams in the T-μ_I plane are shown schematically in Fig. 1. In the second-order scenario, shown on the left, a transition line, corresponding to pseudo-critical behavior for
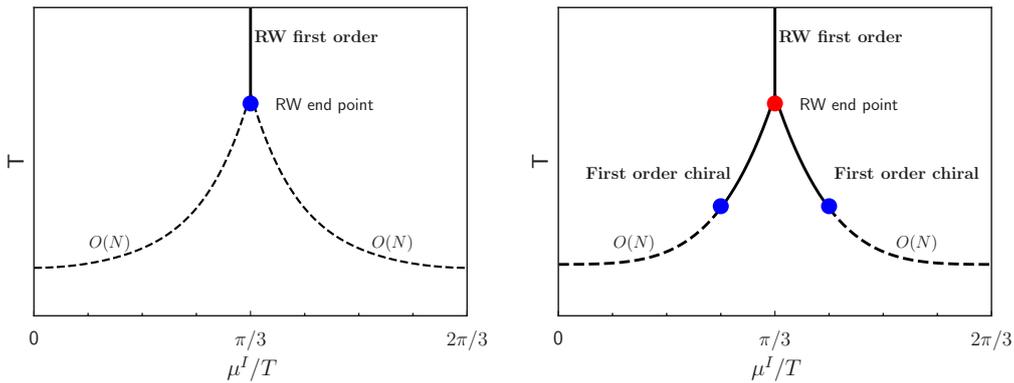
Figure 1: Two possible phase diagrams in the T-μ_I plane at $m_l = 0$. In both cases the vertical line at high temperature is a first-order line at μ_{RW}. *Left*: An O(N) line emerges from $\mu_I = 0$, terminating at a $\mathbb{Z}_2$ point, indicated in blue. *Right*: An O(N) line emerges from $\mu_I = 0$, terminating again at a $\mathbb{Z}_2$ point. This time, the transition continues as a first-order line, until terminating at a first-order triple point, indicated in red.

any non-zero value of the light quark masses and a phase transition in the $O(N)$ universality class for vanishing light quark masses, starts at $\mu_I = 0$ and terminates at a $\mathbb{Z}_2$ end point on the RW plane. By contrast in the first-order scenario, the RW endpoint must be first-order triple; a possible way this could happen is shown on the right. In this case the line of first order phase transitions emerging from the triple-point corresponds to genuine first order chiral phase transitions and with decreasing quark mass values this region in parameter space could extend all the way down to $\mu_I = 0$.

These proceedings give the current status of our ongoing work [10, 11] investigating these aspects of the chiral transition from the perspective of the RW plane.

2. Renormalization group setup

Roberge and Weiss argued that the QCD partition function at imaginary chemical potential is symmetric in μ_I about μ_{RW} [8]. This corresponds to a $\mathbb{Z}_2$ symmetry that may spontaneously break above a critical temperature T_{RW}. We define the physical lattice volume $V = (N_\sigma^3 a)$ and the temperature $T = 1/(N_\tau a)$, where a is the lattice spacing. The Polyakov loop on an $N_\sigma^3 \times N_\tau$ lattice is given by

$$P = \frac{1}{3N_\sigma^3} \sum_{\vec{x}} \text{tr} \prod_\tau U_4(\vec{x}, \tau) \,. \tag{2}$$

The imaginary part of P changes sign under $U \rightarrow U^\dagger$, while the QCD action remains unchanged; hence $\langle \text{Im}\, P \rangle$ can be used as an order parameter for the RW transition at $T = T_{RW}$ and $\mu_I = \mu_{RW}$. In an effective Hamiltonian written near this critical endpoint, $\text{Im}\, P$ couples to the symmetry-breaking field $h \equiv \mu_I - \mu_{RW}$. Observables that respect the symmetry will couple to the reduced temperature $t \equiv (T - T_{RW})/T_{RW}$.

If this RW endpoint belongs to the 3-d, $\mathbb{Z}_2$ universality class, then in a neighborhood of this point, the logarithm of the partition function can be expressed as

$$f \sim b^{-3} f_s(b^{1/\nu} t/t_0, b^{\beta\delta/\nu} h/h_0, b^{-1} N_\sigma/l_0) + \text{reg.} \tag{3}$$

The first term indicates the singular contribution, written in terms of the scale factor b, universal critical exponents β, δ, and ν, and non-universal scale parameters t_0, h_0, and l_0 as well as T_{RW}. The second term indicates regular contributions, which can be written as a Taylor series in t, h, and N_σ.

In this study, we examine (2+1)-flavor QCD on the RW plane, i.e. for $h = 0$. Since $\langle \text{Im}\, P \rangle$ vanishes at $h = 0$ for all T in a finite volume, one may take as order parameter and corresponding susceptibility

$$M \equiv \langle |\text{Im}\, P| \rangle \qquad \text{and} \qquad \chi_M \equiv N_\sigma^3 \left(\langle |\text{Im}\, P|^2 \rangle - \langle |\text{Im}\, P| \rangle^2 \right) \,. \tag{4}$$

Furthermore since $h = 0$, if we set $b = N_\sigma/l_0$, eq. (3) simplifies, and one can derive the scaling behavior

$$M(T, V) = A N_\sigma^{-\beta/\nu} f_{G,L}(z_f) + \text{reg.},$$
$$\chi_M(T, V) = A^2 N_\sigma^{\gamma/\nu} f_{\chi,L}(z_f) + \text{reg.}, \tag{5}$$

3

where $f_{G,L}$ and $f_{\chi,L}$ are finite size scaling functions for the order parameter and susceptibility [12] that depend on the finite size scaling variable[1] $z_f = z_0 N_\sigma^{1/\nu}$ and γ is another critical exponent. In addition, we calculate the Binder cumulant [13]

$$B_4 \equiv \frac{\langle \text{Im}\, P^4 \rangle}{\langle \text{Im}\, P^2 \rangle^2}, \tag{6}$$

which, near the critical point, is just a ratio f_B of scaling functions,

$$B_4(T, V) = f_B(z_f) + \text{reg}. \tag{7}$$

In the chiral limit, a chiral phase transition occurs for all μ_I. To probe this transition, one can use the renormalization-group-invariant order parameter,

$$\Delta_{ls} = \frac{2}{f_K^4} \left(m_s \langle \bar{\psi}\psi \rangle_l - m_l \langle \bar{\psi}\psi \rangle_s \right), \tag{8}$$

where f_K is the kaon decay constant, the chiral condensate for quark flavor f is

$$\langle \bar{\psi}\psi \rangle_f = \frac{1}{4N_\sigma^3 N_\tau} \left\langle \text{tr}\, M_f^{-1} \right\rangle, \tag{9}$$

and M_f is the corresponding staggered fermion matrix. A chiral pseudocritical temperature T_{pc} at nonzero m_l is defined by the peak as a function of T in the disconnected part of the chiral susceptibility

$$\chi^{\text{disc}} = \frac{m_s^2}{4N_\sigma^3 N_\tau f_K^4} \left(\langle (\text{tr}\, M_l^{-1})^2 \rangle - \langle \text{tr}\, M_l^{-1} \rangle^2 \right). \tag{10}$$

This is only a part of the total chiral susceptibility; nevertheless peaks as a function of temperature for χ^{disc} and the total susceptibility will coincide in the chiral limit.

In a neighborhood of T_{RW}, the observables in eq. (8) and (10) will be affected by the RW transition. The chiral condensate and susceptibility are even under $U \to U^\dagger$ and are thus expected to scale as an energy density and specific heat, respectively. Similarly $m_l > 0$ does not break the $\mathbb{Z}_2$ symmetry corresponding to the RW transition, and is therefore an energy-like coupling. In particular this leads to the expectation that χ^{disc} will diverge in the infinite volume limit as

$$\chi^{\text{disc}}(T, V) \sim N_\sigma^{\alpha/\nu} f_{f,L}''(z_f), \tag{11}$$

where $\alpha = 2 - d\nu$ is another 3-d, $\mathbb{Z}_2$ critical exponent and primes indicate derivatives w. r. t. z_f.

3. Computational setup

We perform our calculations using $(2 + 1)$-flavor QCD with HISQ fermions and the tree-level improved Symanzik gauge action. We keep m_s fixed to its physical value and vary m_l between $m_l = m_s/27$ to $m_s/320$, which corresponds to a Goldstone pion mass between 135 and 40 MeV. All lattices have $N_\tau = 4$ and a finite imaginary chemical potential $\mu/T = \pi/3$ for all quark flavors, i.e. we work on the first RW-plane. A summary of simulation parameters is given in Table 1 of Ref. [11]. We set the scale at finite lattice spacing using the parameterization of the line of constant physics given in Ref. [14, 15].

---

[1]We choose $l_0 = 1$, so $z_0 = 1/t_0$.
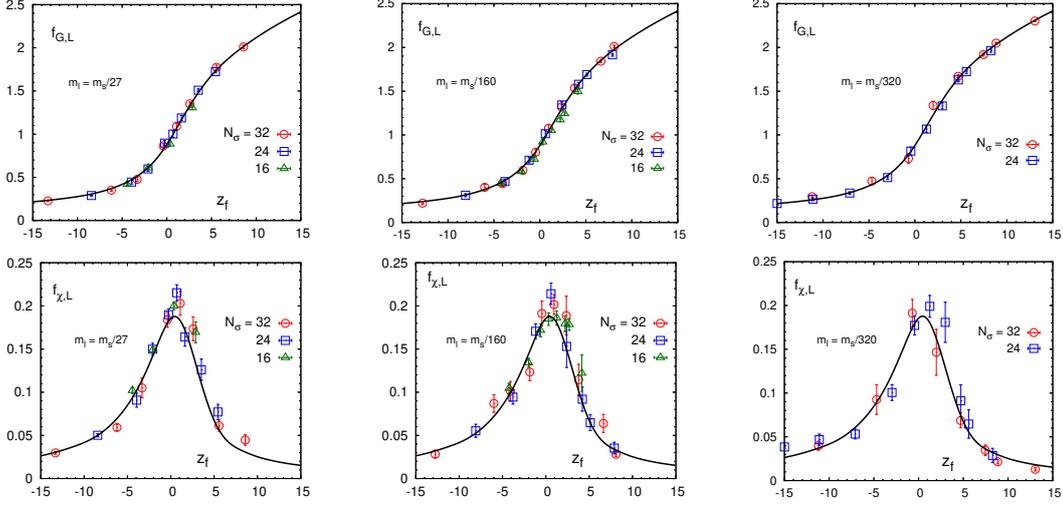
Figure 2: Plots of finite size scaling functions for M (upper row) and χ_M (lower row). From left to right, columns give results for light quark masses $m_s/27$, $m_s/160$, and $m_s/320$. We subtract from χ_M the regular contribution, then data for both M and χ_M are re-scaled according to eq. (13) to isolate the scaling functions. Black, solid lines are the universal scaling functions obtained from 3-d improved Ising model calculations.

m_l	A	T_{RW} [MeV]	z_0	a_0	a_1	χ^2/d.o.f.
$m_s/27$	0.1047(12)	201.05(93)	-1.126(33)	0.072(22)	2.00(31)	2.46
$m_s/160$	0.0947(13)	195.80(11)	-1.073(35)	0.107(25)	2.11(44)	1.60
$m_s/320$	0.0928(16)	194.97(17)	-1.026(30)	0.145(34)	2.12(49)	1.70

Table 1: Summary of fit parameter results for the joint fit given by eq. (13). Temperature ranges for the fits in MeV are [191, 213], [186, 206], and [181, 202] for $m_s/27$, $m_s/160$, and $m_s/320$, respectively.

4. Results

For the critical exponents α, β, γ, and ν we use [16]

$$\alpha = 0.1088, \quad \beta = 0.3258, \quad \gamma = 1.2396, \quad \text{and} \quad \nu = 0.6304. \tag{12}$$

Following the scaling behavior eq. (5) and eq. (6), we employ for M, χ_M, and B_4 the ansätze

$$
\begin{aligned}
M &= A N_\sigma^{-\beta/\nu} f_{G,L}(z_f) \,, \\
\chi_M &= A^2 N_\sigma^{\gamma/\nu} f_{\chi,L}(z_f) + a_0 + a_1 t \,, \\
B_4 &= f_B(z) \,.
\end{aligned}
\tag{13}
$$

We have included the leading regular corrections for χ_M that respect the $\mathbb{Z}_2$ symmetry. This ansatz then corresponds to a five-parameter fit in the non-universal parameters A, T_{RW}, and z_0 as well as the leading regular coefficients a_0 and a_1. We perform first a joint fit for the scaling functions $f_{G,L}$ and $f_{\chi,L}$. The results for z_0 and T_{RW} are then plugged into f_B, which serves as a consistency check. All fits use $N_\sigma \geq 24$ to reduce the effects of regular terms and corrections-to-scaling, and we use a temperature range approximately $T_{\mathrm{RW}} \pm 10$ MeV.
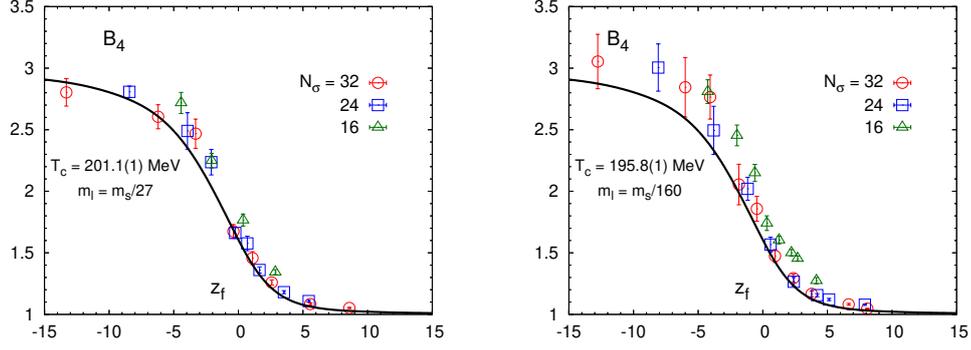
Figure 3: Finite size scaling plots for B_4 for $m_s/27$ (left) and $m_s/160$ (right).
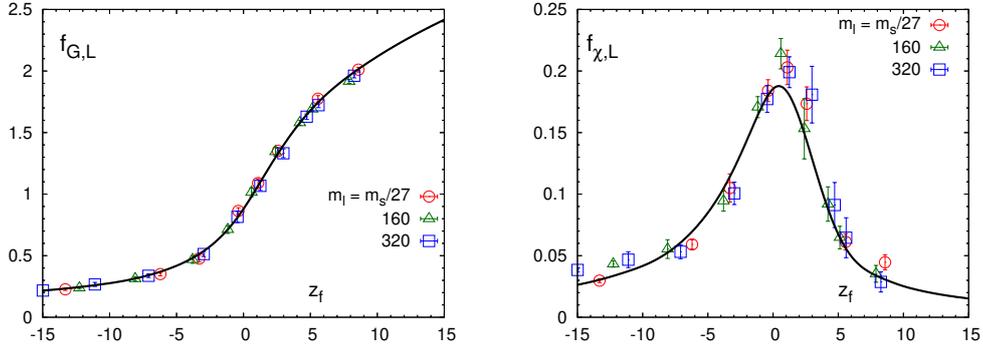
Figure 4: Finite size scaling plots for re-scaled M and χ_M at fixed $N_\sigma = 24$ for different m_l. The universal scaling function is displayed as a black curve.

In Fig. 2 we show the results of our finite size scaling fits plotted against the finite size scaling variable z_f. The top row shows fits for the $f_{G,L}$ and the bottom row shows fits for $f_{\chi,L}$, and each column shows the result for the fits at different quark masses. We subtract the regular part from the χ_M data, then re-scale both M and χ_M to represent only the universal part as defined in eq. (13). The universal functions are based on an improved 3-d Ising model calculation and indicated by the solid, black curves. Results for fit parameters are given in Table 1. T_{RW} exhibits a statistically significant dependence on m_l, decreasing with decreasing m_l. In Fig. 2 we see good agreement with the 3-d, $\mathbb{Z}_2$ expectation and no evidence of a first-order transition down to $m_l = m_s/320$. Fit results for B_4 are shown in Fig. 3. The fits fall near the data, serving as a consistency check.

Results for the re-scaled M and χ_M at fixed $N_\sigma = 24$ down to $m_l = m_s/320$ are shown in Fig. 4. $\mathbb{Z}_2$ scaling fits are shown as black curves. As can be seen in these plots, the data are consistent with the 3-d, $\mathbb{Z}_2$ scaling functions down to $m_l = m_s/320$, showing no evidence for first-order behavior even at our smallest pion mass at approximately 40 MeV. Our results are consistent with the findings of ref. [17].

4.1 Interplay between RW and chiral transition

Finally we turn to the sensitivity of chiral observables to the RW transition. In Fig. 5 (left) we show χ^{disc} at $m_l = m_s/160$. Instead of a slight decrease of peak height with increasing N_σ, which

m_l/m_s	$T_{\text{infl.}}^{\Delta_{ls}}$ [MeV]	$T_{\text{peak}}^{\chi^{\text{disc}}}$ [MeV]
1/27	202.6(7)	202.6(2)
1/160	196.7(6)	197.3(2)
1/320	195.9(7)	194.6(6)

Table 2: Chiral pseudocritical temperatures as determined by the location of the inflection point in Δ_{ls} and peak in χ^{disc} for the largest available volume $N_\sigma = 32$.
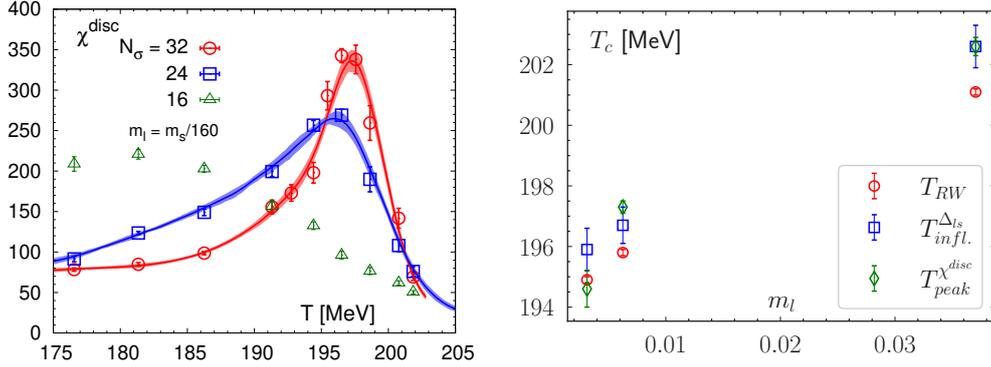
Figure 5: Interplay between RW transition and chiral transition. *Left:* Dependence of χ^{disc} on N_σ at $m_l = m_s/160$. *Right:* T_{RW} from Table 1 and T_{pc} coming from the inflection point in Δ_{ls} and the peak in χ^{disc} against m_l.

is what one would expect from O(N) models, there is instead an increase with N_σ, which is what one expects from eq. (11) in the vicinity of a critical point controlled by the 3-d, $\mathbb{Z}_2$ universality class. In Fig. 5 (right) we show the T_{RW} obtained from fitting the $\mathbb{Z}_2$ scaling functions as listed in Table 1 along with pseudocritical temperatures extracted using the Δ_{ls} inflection point and the χ^{disc} peak at our largest available volume $N_\sigma = 32$ given in Table 2. There is a clear separation of temperatures at our largest m_l, but at the smallest m_l they are statistically compatible. This may hint that the RW and chiral transitions coincide. In that case, a larger symmetry group and universality class would be relevant.

5. Summary and outlook

The RW endpoint appears consistent with the 3-d, $\mathbb{Z}_2$ universality class down to $m_\pi \approx 40$ MeV, and calculations at imaginary μ set an upper bound $m_{\text{crit}} \leq 40$ MeV also for a possible regime of first-order transitions in (2+1)-flavor QCD at vanishing chemical potential. The O(N) and $\mathbb{Z}_2$ transitions may coincide in the chiral limit, resulting in a universality class different from both $\mathbb{Z}_2$ and O(N).

7

Acknowledgements

References

[1] R. D. Pisarski and F. Wilczek, *Remarks on the chiral phase transition in chromodynamics*, *Phys. Rev. D* **29** (1984) 338.

[2] H.-T. Ding et al. [HotQCD collaboration], *Chiral phase transition temperature in (2+1)-flavor QCD*, *Phys. Rev. Lett.* **123** (2019) 062002 [1903.04801].

[3] D. A. Clarke, O. Kaczmarek, A. Lahiri and M. Sarkar, *Sensitivity of the Polyakov loop to chiral symmetry restoration*, *Acta Phys. Polon. Supp.* **14** (2021) 311 [2010.15825].

[4] D. A. Clarke, O. Kaczmarek, F. Karsch, A. Lahiri and M. Sarkar, *Sensitivity of the Polyakov loop and related observables to chiral symmetry restoration*, *Phys. Rev. D* **103** (2021) L011501 [2008.11678].

[5] F. Karsch, E. Laermann and C. Schmidt, *The chiral critical point in three-flavor QCD*, *Phys. Lett. B* **520** (2001) 41 [hep-lat/0107020].

[6] F. Cuteri, O. Philipsen and A. Sciarra, *On the order of the QCD chiral phase transition for different numbers of quark flavours*, *JHEP* **11** (2021) 141 [2107.12739].

[7] A. Bazavov, H.-T. Ding, P. Hegde, F. Karsch, E. Laermann, S. Mukherjee et al., *Chiral phase structure of three flavor QCD at vanishing baryon number density*, *Phys. Rev. D* **95** (2017) 074505 [1701.03548].

[8] A. Roberge and N. Weiss, *Gauge theories with imaginary chemical potential and the phases of QCD*, *Nuclear Physics B* **275** (1986) 734.

[9] C. Bonati, P. de Forcrand, M. D'Elia, O. Philipsen and F. Sanfilippo, *Chiral phase transition in two-flavor QCD from an imaginary chemical potential*, *Phys. Rev. D* **90** (2014) 074030 [1408.5086].

[10] J. Goswami, F. Karsch, A. Lahiri and C. Schmidt, *QCD phase diagram for finite imaginary chemical potential with HISQ fermions*, *PoS(LATTICE2018)* (2018) 162 [1811.02494].

[11] J. Goswami, F. Karsch, A. Lahiri, M. Neumann and C. Schmidt, *Critical end points in (2+1)-flavor QCD with imaginary chemical potential*, *PoS(CORFU2018)* (2019) 162 [1905.03625].

[12] J. Engels, L. Fromme and M. Seniuch, *Numerical equation of state from an improved three-dimensional Ising model*, *Nucl. Phys. B* **655** (2003) 277 [cond-mat/0209492].

[13] K. Binder, *Finite size scaling analysis of ising model block distribution functions*, *Z. Phys. B* **43** (1981) 22.

[14] A. Bazavov et al. [HotQCD collaboration], *The chiral and deconfinement aspects of the QCD transition*, *Phys. Rev. D* **85** (2012) 054503 [1111.1710].

[15] D. Bollweg et al. [HotQCD collaboration], *Second order cumulants of conserved charge fluctuations revisited: Vanishing chemical potentials*, *Phys. Rev. D* **104** (2021) 074512 [2107.10011].

[16] J. Zinn-Justin, *Precise determination of critical exponents and equation of state by field theory methods*, *Phys. Rept.* **344** (2001) 159 [hep-th/0002136].

[17] C. Bonati, E. Calore, M. D'Elia, M. Mesiti, F. Negro, F. Sanfilippo et al., *Roberge-Weiss endpoint and chiral symmetry restoration in $N_f = 2 + 1$ QCD*, *Phys. Rev. D* **99** (2019) 014502 [1807.02106].